Stabilization of Iron Oxide Nanoparticles in High Sodium and Calcium Brine at High Temperatures with Adsorbed Sulfonated Copolymers

Hitesh G. Bagaria[a], KiYoul Yoon[a], Bethany M. Neilson[b], Victoria Cheng[a], Jae Ho Lee[a], Andrew J. Worthen[a], Zheng Xue[a], Chun Huh[c], Steven L. Bryant[c], Christopher W. Bielawski[b] and Keith P. Johnston[a]

[a]Department of Chemical Engineering, [b]Department of Chemistry and Biochemistry, [c]Department of Petroleum and Geosystems Engineering, The University of Texas at Austin, TX 78712

Supporting Information

MATERIALS AND METHODS

Iron(II) chloride tetrahydrate, iron (III) chloride hexahydrate, citric acid monohydrate, and 30% ammonium hydroxide were obtained from Sigma-Aldrich and used as received. The monomers *t*-butyl acrylate (*t*BA) and styrene were purchased from commercial sources and filtered through a short plug of basic alumina to remove the 4-methoxyphenol (MEHQ) stabilizer and were degassed by bubbling with dry nitrogen for 15 min prior to use. N,N,N',N',N-pentamethyldiethylenetriamine, ethyl 2-bromoisobutyrate, acrylic acid, potassium persulfate, and sodium metabisulfite were obtained from commercial sources and used as received. The monomer 2-amino-2-methylpropanesulfonate (AMPS) was a gift from Lubrizol corporation and used as received.

Nucelar Magnetic Resonance Spectroscopy (NMR). ^{1}H NMR spectra were recorded using a Varian 400 MHz spectrometer. Chemical shifts δ (in ppm) are referenced to tetramethylsilane using the residual solvent as an internal standard: $CDCl_3$, 7.24 ppm; D_2O, 4.79 ppm.

Infrared Spectroscopy (IR). IR spectra were recorded on a Thermo Scientific Nicolet iS5 spectrometer with an iD3 attenuated total reflectance (ATR) attachment (Ge crystal).

Gel permeation chromatography (GPC). GPC analysis was performed on a Viscotek system equipped with a VE 1122 pump, a VE 7510 degasser, two fluorinated polystyrene columns (IMBHW-3078 and I-MBLMW-3078) thermostated to 30 °C (using a ELDEX CH 150 column heater) and arranged in series, using refractive index (RI) detection. Molecular weight and polydispersity data are reported relative to polystyrene standards in tetrahydrofuran (THF).

Synthesis of poly(2-acrylamido-3-methylpropanesulfonate-co-acrylic acid) (poly(AMPS-*co*-AA)). Generally, a three-necked round bottom flask equipped with a magnetic stir bar, a nitrogen inlet and a reflux condenser was charged with AMPS monomer, potassium persulfate and sodium metabisulfite under an atmosphere of nitrogen. The flask was sealed with rubber septa and deionized water that was previously degassed by bubbling with nitrogen for 30 min was added via a nitrogen-purged syringe or a cannula to the reaction flask, such that the concentration of AMPS monomer was 1.0 M. With stirring, acrylic acid was added to the reaction flask via a nitrogen-purged syringe. The flask was placed in an oil bath and stirred at 80 °C for 16 h. The reaction mixture was then cooled to room temperature and the water was removed under reduced pressure. The resulting white solid was dried under reduced pressure until a constant mass was reached. ^{1}H NMR (400 MHz, D_2O): δ 1.46-1.80 (m, br, 10H), 2.22 (br, 2H), 3.32 (br, s, 2H). IR (ATR): ν 2943.1, 1719.9, 1654.7, 1555.6, 1455.9, 1173.7, 1040.9, 884.4, 850.1.

Synthesis of poly(t-butyl acrylate)-block-(styrene) (PtBA-b-PS). Under an atmosphere of nitrogen an oven-dried 50 mL Schlenk flask with a magnetic stir bar was charged with 300 mg (2.1 mmol) of copper(I) bromide. The flask was sealed with a rubber septum secured with copper wire and was

evacuated and back-filled with nitrogen three times before 5 mL (34.1 mmol) of *tert*-butyl acrylate was added via a gas-tight syringe that had been purged with nitrogen. After one freeze-pump-thaw cycle, 0.5 mL (2.4 mmol) of *N,N,N′,N′,N*-pentamethyldiethylenetriamine was added via a nitrogen-purged gas-tight syringe. After a second freeze-pump-thaw cycle, 0.1 mL (0.68 mmol) of ethyl-2-bromoisobutyrate was added via a gas-tight syringe that had been purged with nitrogen. After two more freeze-pump-thaw cycles, the reaction mixture was allowed to return to ambient temperature, and the reaction flask was backfilled with nitrogen and placed in an oil bath at 50 °C. The reaction mixture was allowed to stir for 3 h at the same temperature, after which an aliquot was removed from the reaction and analyzed by GPC (M_n = 5,500, M_w/M_n = 1.15) prior to addition of 7.4 mL (64.5 mmol) of styrene. The reaction mixture was allowed to stir for a further 18 h at 50 °C, then was cooled to room temperature. The mixture was then taken up into THF and passed through a plug of neutral alumina to remove the metal/ligand catalyst system. The resulting polymer solution was concentrated and purified by precipitation into a mixture of methanol and water (1/1, v/v). ^{1}H NMR (400 MHz, D_2O): δ 1.42-1.50 (m, br, 13H), 1.83 (br, 2H), 2.21 (br, s, 1H), 6.44-6.57 (br, d, 3H), 6.98-7.08 (br, d, 5H). GPC: M_n = 17,055 Da, M_w/M_n = 1.29.

Synthesis of poly(sytrenesulfonate-b-acrylic acid) poly(SS-*b*-AA) (2.4 : 1). A 1 L round bottom flask was charged with P*t*BA-PS (prepared in the previous step) dissolved in 300 mL of chloroform. In a separate flask with a stir bar, a solution of 66 mL of acetic anhydride in 100 mL of chloroform was cooled to 0 °C. Concentrated sulfuric acid (37 mL) was added dropwise and the mixture was stirred at 0 °C for an additional 10 min before it was added to the flask containing the polymer solution. The reaction mixture was heated to 60 °C and stirred for 16 h, then was cooled to room temperature and slowly poured into methanol. The solution was neutralized by slow addition of 3.0 M NaOH, and the organic solvents were removed under reduced pressure. The resulting aqueous solution was loaded into dialysis tubing and dialyzed against DI H_2O for 3 days. After dialysis the desired polymer was isolated as an orange glassy solid by concentration and drying under reduced pressure (11.0 g, 46% yield over 2 steps). ^{1}H NMR (400

MHz, D_2O): δ 1.2-2.2 (m, br, 10H), 3.65 (br, 1H), 6.69 (br, s, 4H), 7.59 (br, s, 4H). IR (ATR): v 3390.9, 2945.9, 1715.5, 1568.6, 1455.0, 1410.9 1221.1, 1132.5, 1049.5, 1006.2, 946.2, 775.4.

Synthesis of citrate-coated IO nanoclusters. Citrate-coated iron oxide nanoclusters were prepared by coprecipitation of Fe(II) and Fe(III) chlorides in an alkaline solution[1-4]. Briefly, a mixture of 0.86 g $FeCl_2$ and 2.35 g $FeCl_3$ (1:2 molar ratio) and 0.05 g of citric acid, which correspond to a citrate/total-Fe molar ratio = 0.018,[5] were dissolved in 40 mL DI water. The solution was magnetically stirred for 10 min under ambient atmosphere. The mixture was heated to 90 °C while stirring and 10 mL of 30 wt% aqueous NH_4OH solution was injected to nucleate the iron oxide nanoparticles (NPs). The NP growth was continued for 2 h at 90 °C. The mixture was then cooled to room temperature, centrifuged and dispersed in 20 mL of DI water with a Branson probe sonication microtip. These particles were termed as 'low Cit-IO'. After separating the particles again (6000 g, 10 min), additional citrate groups were introduced by probe sonication of the pellet in 20 mL of citric acid solution (20 mg/ml, pH = 5) for 15 min. Upon removal of large aggregates (7000 g, 10 min), the supernatant was centrifuged at 10000 g for 20 min to recover a pellet of citrate-stabilized IO nanoclusters that were dispersed in 25 mL of DI water. The final dispersion contained ~2.5 - 3 wt% IO, as observed by flame atomic absorption spectroscopy (FAAS) suggesting an IO yield of ~60-70%. These citrate-IO nanoclusters with the higher citrate level were the primary platform particles for the coating experiments.

Scheme S1. Synthesis of poly(AMPS-*co*-AA) via aqueous radical polymerization.

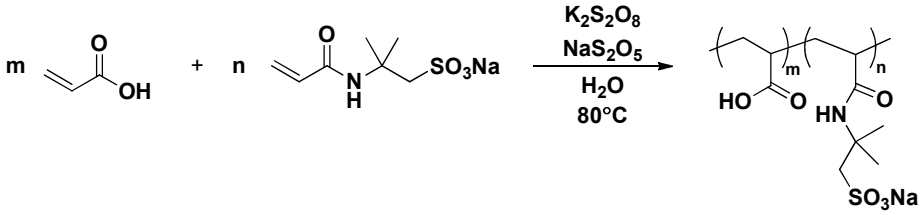

Scheme S2. Synthesis of poly(SS-*b*-AA)via ATRP followed by sulfonation and deprotection.

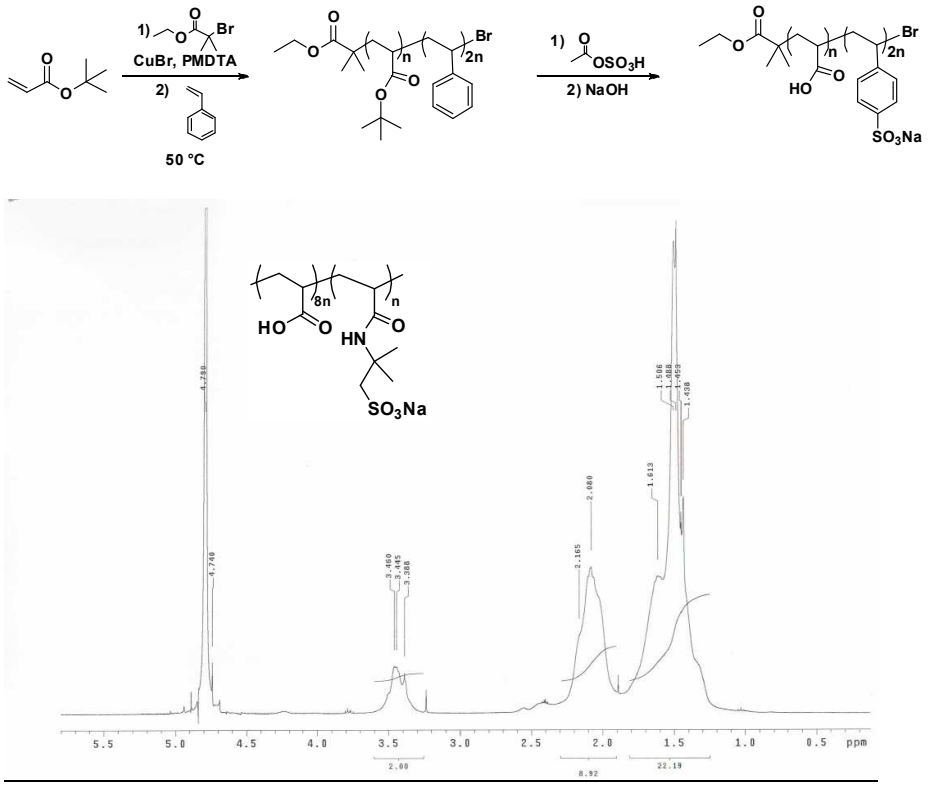

Figure S1. ^{1}H NMR spectrum of poly(AMPS-*co*-AA) (1:8) (D_2O).

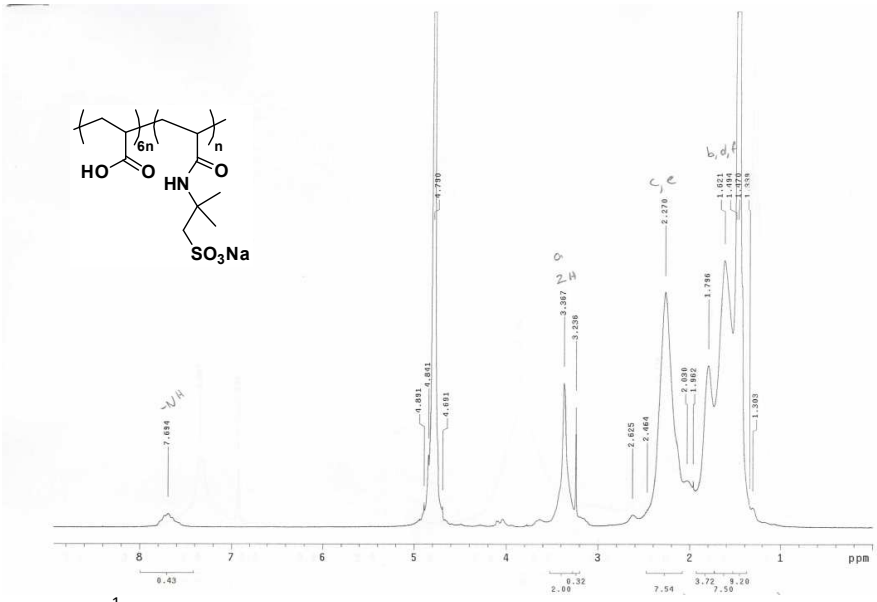

Figure S2. ^{1}H NMR spectrum of poly(AMPS-*co*-AA) (1:6) (D_2O).

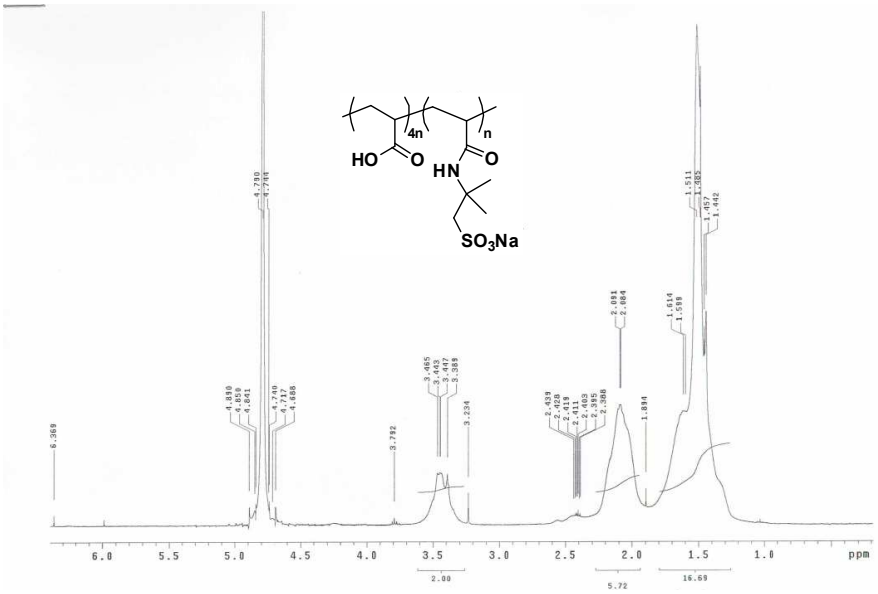

Figure S3. ^{1}H NMR spectrum of poly(AMPS-*co*-AA) (1:4) (D_2O).

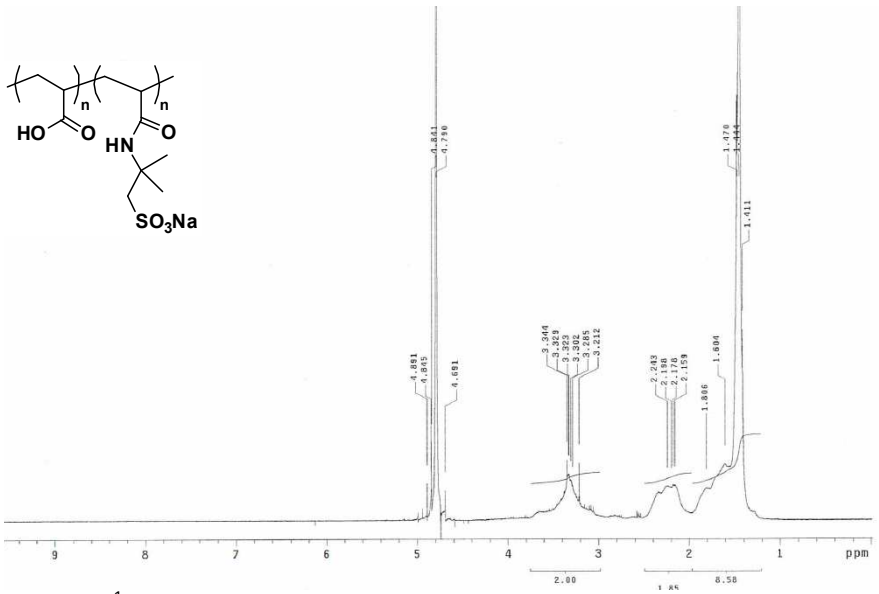

Figure S4. ^{1}H NMR spectrum of poly(AMPS-*co*-AA) (1:1)-212 (D_2O).

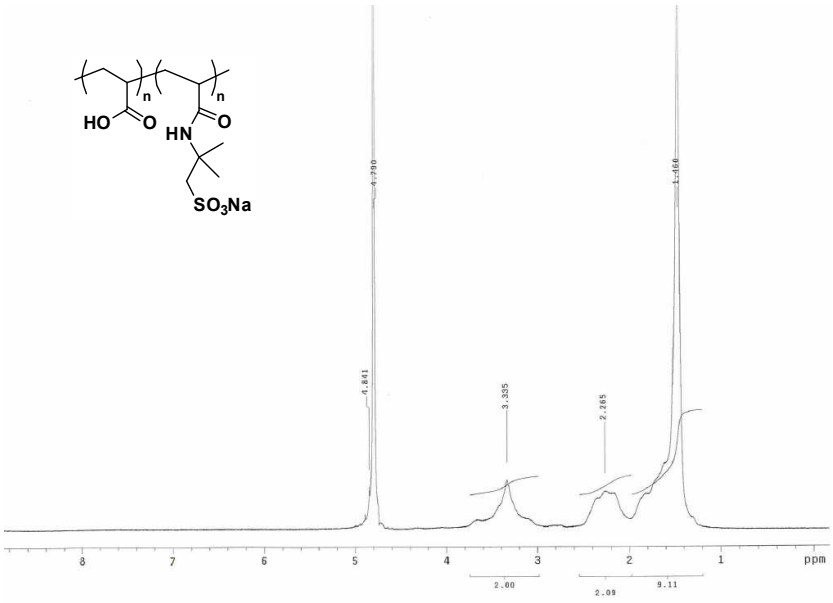

Figure S5. ^{1}H NMR spectrum of poly(AMPS-*co*-AA) (1:1)-52 (D_2O).

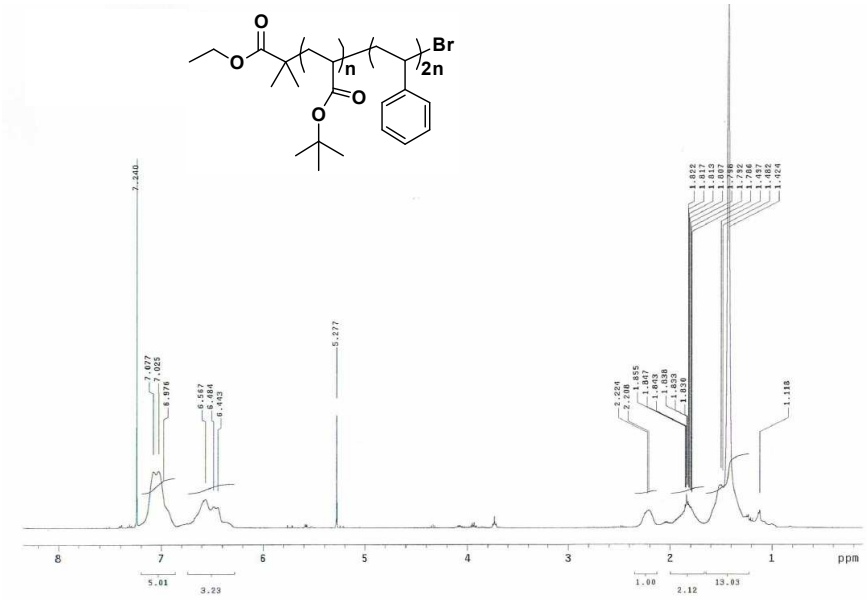

Figure S6. ^{1}H NMR spectrum of P*t*BA-PS ($CDCl_3$).

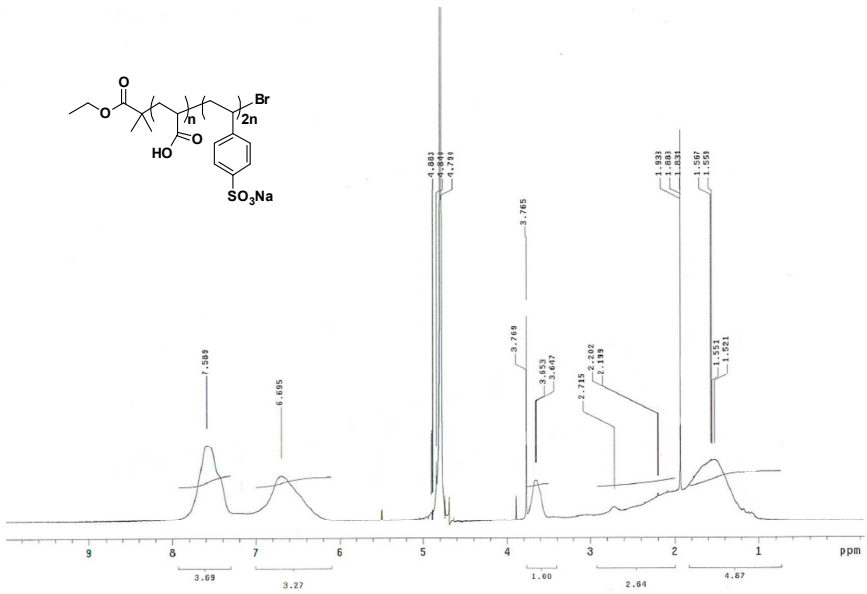

Figure S7. ^{1}H NMR spectrum of poly(SS-*b*-AA) (2.4 : 1) (D_2O).

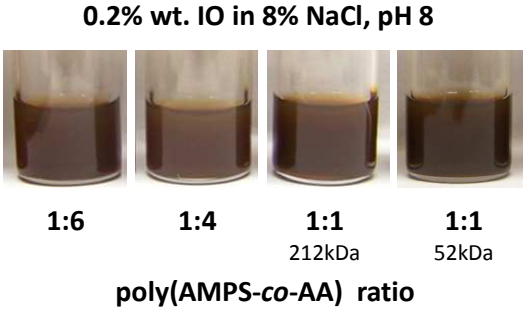

Figure S8. poly(AMPS-*co*-AA) coated IO dispersions (0.2% wt.) in 8% NaCl, pH = 8 at room temp. were also found to be stable (picture after 1 day). These results suggested that Ca^{2+}-bridge between the polymer and the citrate IO clusters does not undergo ion-exchange with Na^{+}.

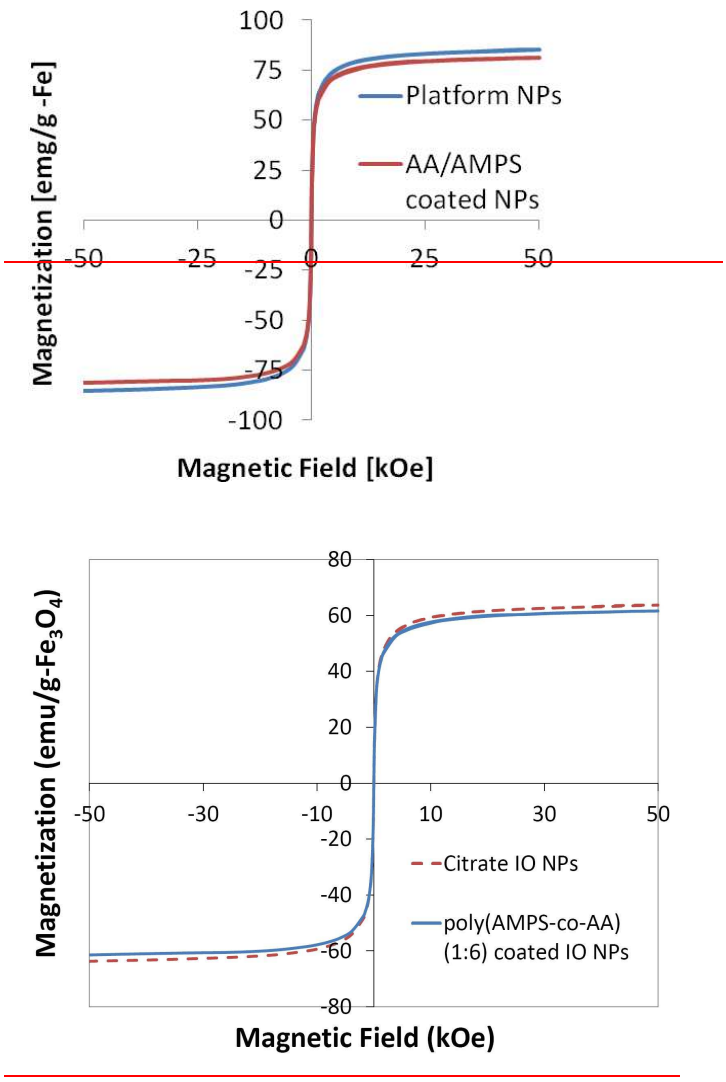

Figure S9. Magnetization of Cit-IO nanoclusters before and after poly(AMPS-*co*-AA) (1:6) coating.

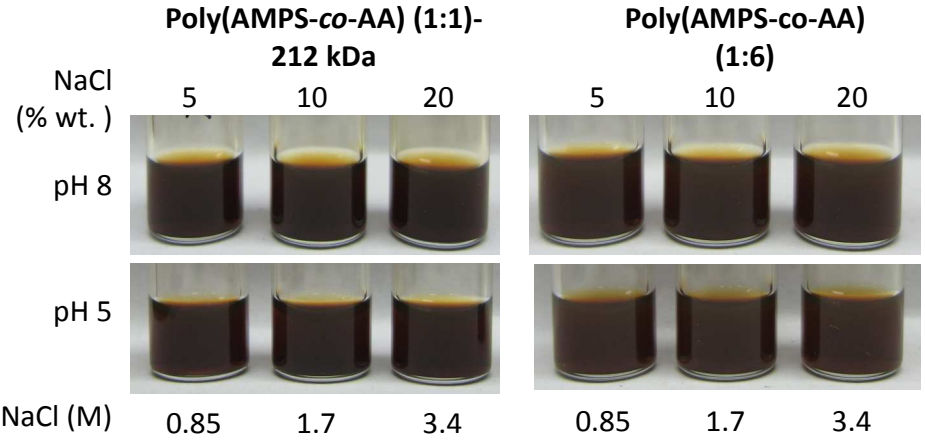

Figure S10. Stability of IO coated with poly(AMPS-*co*-AA) (1:1)-212 and poly(AMPS-*co*-AA) (1:6) after 3 months in NaCl solutions up to 20% wt. NaCl (3.4 M) at the indicated pH values and 0.2% wt. IO conc. All dispersions were found to be stable.

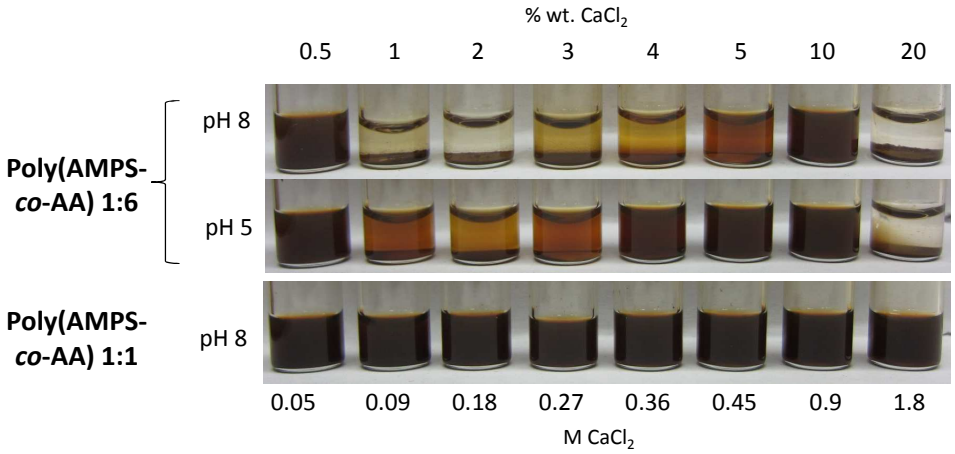

Figure S11. Stability of IO coated with poly(AMPS-*co*-AA) (1:6) and poly(AMPS-*co*-AA) (1:1)-212 after 3 months in $CaCl_2$ solutions of various concentrations (indicated) at the given pH values. poly(AMPS-*co*-AA) (1:1) coated IO clusters at pH = 5 (not shown) were similar to the above dispersions at pH = 8. poly(AMPS-*co*-AA) (1:1) IOs remained stable even after 3 months.

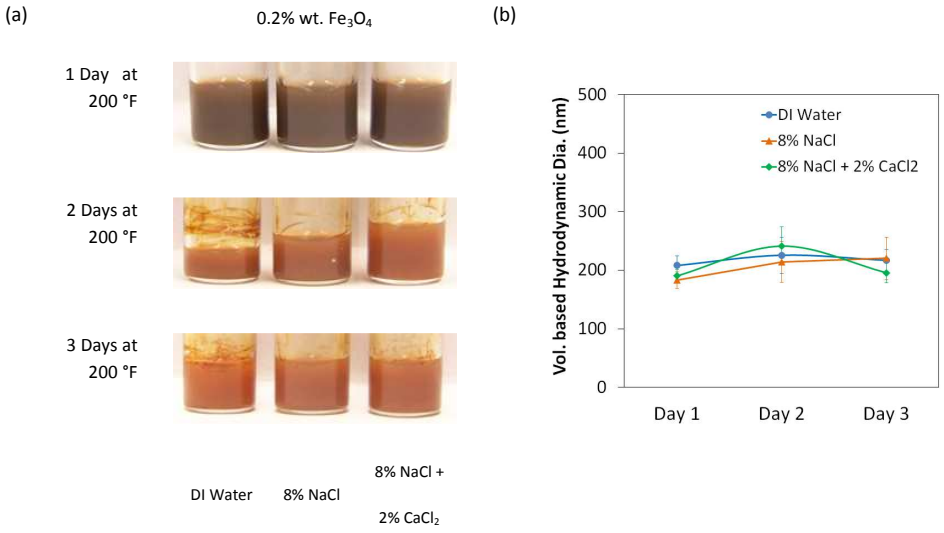

Figure S12. Colloidal stability of poly(SS-*b*-AA) (2.4 : 1) coated IO clusters in various saline conditions as evidenced by photos of dispersions and hydrodynamic diameters measured by DLS (*Note: On Day 2, vials were topped with DI water to replenish water lost by evaporation*).

Additional Steric Stabilization Literature:

Various studies have examined steric stabilization of nanoparticles in salt solutions using relatively low MW non-ionic polymers, especially PEG, for cores smaller than 10 nm, where vdW forces are much more easily overcome. The cloud point temperature of PEG, above which it precipitates, decreases with MW and salinity, and thus it is most effective at very low MWs. CdSe/ZnS quantum dots (8.4 nm) and IO NPs (9.6 nm) synthesized with oleic acid ligands followed by coating with amphiphilic PEG on individual NPs led to stability in 1 M and 2 M NaCl, respectively.[6] Phosphonate-terminated PEG (EO = 10)[7, 8] was adsorbed on naked 7 nm ceria and 7.1 nm maghemite NPs for stability in 1 M NaCl.[8] Ligand exchange with catechol-terminated PEG (EO = 14-17) led to stable dispersions of Au NPs (10 nm) and CdSe/ZnS QDs (~10 nm) in 2 M NaCl, and IO NPs (11 nm) in 1M NaCl.[9, 10] Other non-ionic polymer stabilizing groups investigated for IO NPs (6-8 nm) include polyacrylamide [11], which imparted stability in 2 M NaCl and saturated NH_4NO_3.

Comment [BN1]: Hitesh: I did not transfer the references in this section from the manuscript because I don't use endnote and didn't want to mess up all the order. They will need to be added here and removed from the manuscript.

HB: this is already taken care of by Endnote

Ohshima's Soft Particle Electrophorectic Mobility Model

The electrophoretic mobility data of poly(AMPS-*co*-AA)(1:1)-212 coated IOs shown in Fig. 5 at various ionic strength of NaCl were fit to the following equations by Ohshima[12-14]:

$$\mu = \frac{\rho_{fix}}{\eta\lambda^2} + \frac{2\varepsilon_r \varepsilon_0}{3\eta}\left(\frac{\psi_0/\kappa_m + \psi_{DON}/\lambda}{1/\kappa_m + 1/\lambda}\right)\left(1 + \frac{1}{2(1+d/a)^3}\right) \quad \text{(S1)}$$

$$\psi_{DON} = \frac{kT}{ze}\ln\left\{\frac{\rho_{fix}}{2zen^{\infty}} + \left[\left(\frac{\rho_{fix}}{2zen^{\infty}}\right)^2 + 1\right]^{0.5}\right\} \quad \text{(S2)}$$

$$\psi_0 = \psi_{DON} + \frac{2n^{\infty}kT}{\rho_{fix}}\left\{1 - \left[\left(\frac{\rho_{fix}}{2zen^{\infty}}\right)^2 + 1\right]^{0.5}\right\} \quad \text{(S3)}$$

$$\kappa = \left(\frac{\varepsilon_r \varepsilon_0 kT}{2en^{\infty}}\right)^{0.5} \quad \text{(S4)}$$

$$\kappa_m = \kappa\left[1 + \left(\frac{\rho_{fix}}{2zen^{\infty}}\right)^2\right]^{0.25} \quad \text{(S5)}$$

where,

μ : electrophoretic mobility in m^2/V-sec, which is fit to the experimental mobility data

ρ_{fix} : charge density of polyelectrolyte groups in C/m^3 – (fit parameter)

η : viscosity of the solution = 9×10^{-4} N-S/m^2

λ^{-1} : Brinkman screening length/ softness of the polyelectrolyte layer – (fit parameter)

ε_r : relative permittivity / dielectric constant of water = 78.5

ε_0 : permittivity of vacuum = 8.85×10^{-12} F/m

ψ_{DON} : Donnan potential due to charges in the polyelectrolyte layer in V (see Table S1)

ψ_0 : surface potential in V (see Table S1)

κ_m : modified inverse Debye length for the polyelectrolyte layer in m^{-1} (see Table S1)

κ : inverse Debye length in m^{-1} (see Table S1)

d : thickness of the polymer layer = 20×10^{-9} nm

a : radius of the core particle = 46.5×10^{-9} nm

k : Boltzmann constant = 1.3806×10^{-23} J/K

T : temperature = 298 K

z : valence of electrolyte ion, for NaCl = 1

e : elementary charge = 1.602×10^{-19} C

n^{∞} : number concentration of ions in bulk solution in m^{-3} (see Table S1)

The values of the fit parameters were found to be

ρ_{fix} = 2.91×10^6 Columbus/m^3 (or) 30.1 mol/m^3 of charge
λ^{-1} = 2.2×10^{-9} m (or) 2.2 nm

The above equations S1-S5 hold good when ka , kd , λd all are >> 1. These conditions are satisfied at high salinity (0.5 M NaCl) and thick polyelectrolye layers in our case (ka =108, kd =47 and λd = 9).

Table S1. Debye lengths, Donnan and Surface potential calculated with equations S1-S5 at various ionic strengths.

Ionic Strength (M)	**Number conc. of ions in bulk n^{∞} (m^{-3})**	**Debye Length κ^{-1} (m)**	**Modified Debye length for polyelectrolyte κ_m^{-1} (m)**	**Donnan Potential ψ_{DON} (mV)**	**Surface Potential ψ_0 (mV)**
0.01	6.0E+24	3.0E-09	2.3E-09	-30.8	-17.0
0.05	3.0E+25	1.4E-09	1.3E-09	-7.6	-3.8
0.1	6.0E+25	9.6E-10	9.6E-10	-3.9	-1.9
0.25	1.5E+26	6.1E-10	6.1E-10	-1.5	-0.8
0.5	3.0E+26	4.3E-10	4.3E-10	-0.8	-0.4
1.8	1.1E+27	2.3E-10	2.3E-10	-0.2	-0.1

Models that account for charge of core particles were also tested [14, 15] with the core citrate IO particles that showed a zeta potential of -31 mV. The fit parameters (below) were found to be the same as with

equations S1-S5 that do not consider the charge of core particles. Similar results with and without considering bare particle surface charge, were likely due to a thick polyelectrolyte layer.

ρ_{fix} = 2.90 × 10^6 Columbus/m^3 (or) 30.0 mol/m^3 of charge
λ^{-1} = 2.2 × 10^{-9} m (or) 2.2 nm

REFERENCES

1. Massart, R., Preparation of aqueous magnetic liquids in alkaline and acidic media. *IEEE Trans. Magn.* **1981,** 17, 1247-1248.
2. Lyon, J. L.; Fleming, D. A.; Stone, M. B.; Schiffer, P.; Williams, M. E., Synthesis of Fe oxide core/Au shell nanoparticles by iterative hydroxylamine seeding. *Nano Letters* **2004,** 4, 719-723. .
3. Ditsch, A.; Laibinis, P. E.; Wang, D. I. C.; Hatton, T. A., Controlled Clustering and Enhanced Stability of Polymer-Coated Magnetic Nanoparticles. *Langmuir* **2005,** 21, (13), 6006-6018.
4. Sahoo, Y.; Goodarzi, A.; Swihart, M. T.; Ohulchanskyy, T. Y.; Kaur, N.; Furlani, E. P.; Prasad, P. N., Aqueous ferrofluid of magnetite nanoparticles: fluorescence labeling and magnetophoretic control. *J. Phys. Chem. B* **2005,** 109, 3879–3885.
5. Bee, A.; Massart, R.; Neveu, S., Synthesis of Very Fine Maghemite Particles. *Journal of Magnetism and Magnetic Materials* **1995,** 149, (1-2), 6-9.
6. Yu, W. W.; Chang, E.; Falkner, J. C.; Zhang, J. Y.; Al-Somali, A. M.; Sayes, C. M.; Johns, J.; Drezek, R.; Colvin, V. L., Forming biocompatible and nonaggregated nanocrystals in water using amphiphilic polymers. *Journal of the American Chemical Society* **2007,** 129, (10), 2871-2879.
7. Qi, L.; Sehgal, A.; Castaing, J. C.; Chapel, J. P.; Fresnais, J.; Berret, J. F.; Cousin, F., Redispersible hybrid nanopowders: Cerium oxide nanoparticle complexes with phosphonated-PEG oligomers. *Acs Nano* **2008,** 2, (5), 879-888.
8. Chanteau, B.; Fresnais, J.; Berret, J. F., Electrosteric Enhanced Stability of Functional Sub-10 nm Cerium and Iron Oxide Particles in Cell Culture Medium. *Langmuir* **2009,** 25, (16), 9064-9070.
9. Palui, G.; Na, H. B.; Mattoussi, H., Poly(ethylene glycol)-Based Multidentate Oligomers for Biocompatible Semiconductor and Gold Nanocrystals. *Langmuir* **2012,** 28, (5), 2761-2772.
10. Bin Na, H.; Palui, G.; Rosenberg, J. T.; Ji, X.; Grant, S. C.; Mattoussi, H., Multidentate Catechol-Based Polyethylene Glycol Oligomers Provide Enhanced Stability and Biocompatibility to Iron Oxide Nanoparticies. *Acs Nano* **2012,** 6, (1), 389-399.
11. Jain, N.; Wang, Y.; Jones, S. K.; Hawkett, B. S.; Warr, G. G., Optimized Steric Stabilization of Aqueous Ferrofluids and Magnetic Nanoparticles. *Langmuir* **2010,** 26, (6), 4465-4472.
12. Ohshima, H., Electrophoretic Mobility of Soft Particles. *Colloids and Surfaces a-Physicochemical and Engineering Aspects* **1995,** 103, (3), 249-255.
13. Ohshima, H., Electrical phenomena in a suspension of soft particles. *Soft Matter* **2012,** 8, (13), 3511.
14. Louie, S. M.; Phenrat, T.; Small, M. J.; Tilton, R. D.; Lowry, G. V., Parameter Identifiability in Application of Soft Particle Electrokinetic Theory To Determine Polymer and Polyelectrolyte Coating Thicknesses on Colloids. *Langmuir* **2012**.
15. Ohshima, H., Electrophoresis of soft particles. *Advances in Colloid and Interface Science* **1995,** 62, (2-3), 189-235.